Microstructural Evolution and Life Evaluation during Creep/Rupture Process of a Single Crystal Superalloy

H. C. Yu, Y. Li

Beijing Institute of Aeronautical Materials, Beijing 100095, China
E-mail: yhcyu@126.com

Abstract: Creep and stress rupture tests were conducted at elevated temperatures on a single crystal nickel base superalloy. Creep process may be divided into different stages, one is initial stage characterized by dislocation slip and the other is rafting one characterized by γ' phase rafting. The rupture results show that the alloy with [001] and [111] orientations exhibit superior rupture strength to that with [011] at 980°C, which may be ascribed to different dislocation slip mechanism, but the difference among stress rupture strength of the alloy with three orientations is relatively small at 1070°C. A damage parameter is deduced on the quantitative relationship between applied stress and basic mechanical properties of the material, i.e. elastic modulus, yield stress and ultimate tensile strength. The model can be used to predict the rupture life of the alloy with any orientation at high temperature. The prediction values agree well with test data.

Keywords: Creep; Life evaluation; Microstructure; Stress rupture; Single crystal nickel base superalloy.

1. Introduction

Single crystal nickel base superalloy is superior to conventionally cast superalloy, because the elimination of grain boundaries enhances elevated temperature ductility and single crystal casting process provides a preferred low modulus [001] texture orientation parallel to the solidification direction. The minor alloying elements used as grain boundary strengtheners and acting to reduce the incipient melting temperature are no longer useful here. These result in a high creep strength and ductility as well as thermal fatigue resistance of the alloy [1, 2]. It also derives its high creep resistance from the design of chemical compositions and its microstructure containing a large volume fraction of γ' phase as precipitated particles. Therefore, single crystal nickel base superalloy is very attractive for use as turbine blade in aero-engine. It allows a higher operating temperature and thus increases the overall efficiency [1].

During service, an important life limiting factor is the creep deformation since single crystal component should withstand gas emerging from the combustion chamber and experience a combination of high temperature and stress. Although the nominal orientation of cast single crystal superalloy blade is generally along <001>, the blade experiences stresses in a variety of orientations due to many factors, for example, the orientation of actual blade may fall in a wide range near the nominal orientation, and the complex cooling system of air channel in the

blade may also result in thermal stress generation in various orientations [3]. Anisotropic creep property of such single crystals should be investigated.

The present study is aimed at the microstructural evolution and the stress rupture property of a low-cost second-generation single crystal nickel base superalloy with three orientations. An approach based on "damage parameter" was discussed to characterize the stress rupture life of the alloy.

2. Material and experimental procedures
2. 1 Material and specimens

The material studied is a single crystal nickel base superalloy with high γ' volume fraction. The chemical compositions (wt%) of the material are 0.01C, 4.4Cr, 9.0Co, 8.0W, 1.8Mo, 5.8Al, 0.6Nb, 7.2Ta, 2.2Re, 0.1Hf and balance Ni. This alloy contains 2 wt% Re and additive refractory element (W, Mo, Ta, Re and Nb) content of about 19.5 wt% [4]. The alloy was directionally solidified along the natural dendrite direction [001] in the form of single crystal cylinder 15mm in diameter and 105mm in length. The same size cylinder was also cast with an axial direction near [011] and [111] corners. The crystal orientation of the round bar was measured by Laue back reflection X-ray technique. The maximum deviation of the rod axis from [001], [011] or [111] direction was laid within 10º. All of the cast bars were fully heat treated, i.e. solution heat treated (1290°C/1h + 1300°C/2h + 1315°C/4h/AC), and ageing heat treated for two stages (1120°C/4h/AC + 870°C/32h/AC).
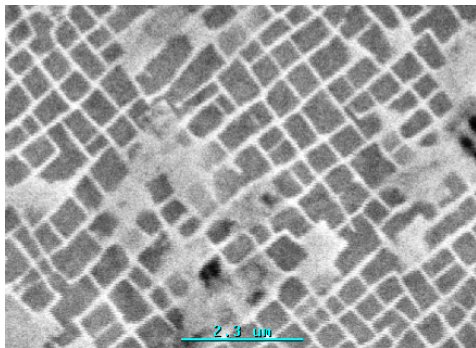
Fig. 1. Microstructure of the alloy   Fig. 2. Young's modulus vs. temperature
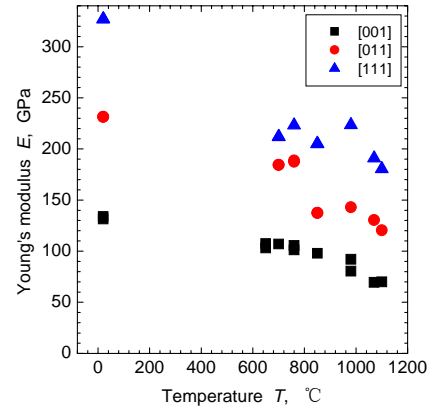
Figure 1 shows a scanning electron microscope (SEM) image of the microstructure of the alloy after heat treatment. The alloy microstructure consists of regularly packed cuboidal γ' particles in a face-centered cubic (fcc) γ matrix. The γ'/γ arrangement in the whole volume is quite regular with the mean size of the γ? particles of about 400 nm. The volume fraction of γ' particles is approximately 65%. The gray areas in Fig. 1 disturbing the regular cuboidal appearance represent horizontal sections right through particular γ matrix channels. The stress rupture specimen was subsequently machined with a gauge length of 25mm and gauge diameter of 5mm as well as a shoulder structure at the

two ends of the specimen to prevent the adhesion with the clamp at higher temperature, its total length is 60mm. The creep specimen was also machined with a gauge length of 25mm, gauge diameter of 5mm and total length of 100mm.
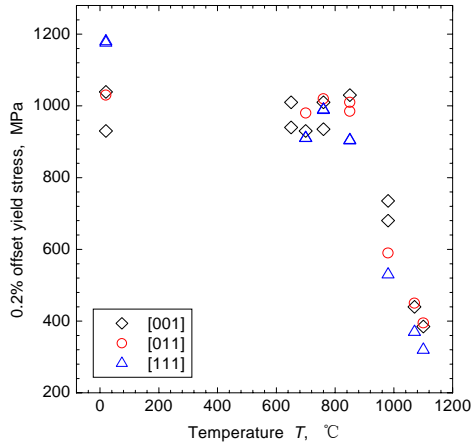
Fig. 3. Yield stress vs. temperature   Fig. 4. *UTS* vs. temperature
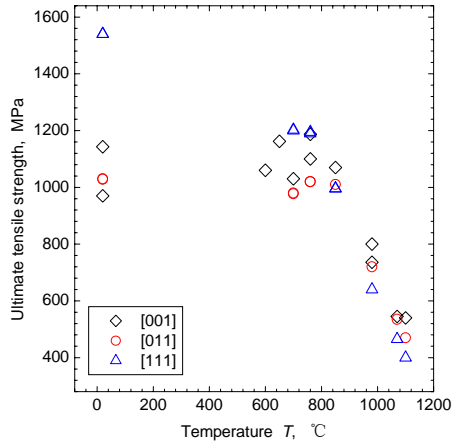
The mechanical properties of the alloy after heat treatment at different temperature were obtained by using standard tensile specimens. The Young's modulus of the alloy decreases with temperature increase for all the three orientation as shown in Fig.2. It is orientation dependent and shows the lowest values with [001] and the highest values with [111] orientation at different temperature. With [001] orientation, the 0.2% offset yield stress is nearly unchanged during temperature changes from room temperature to 760°C. However, when temperature increases to 850°C, it reaches its maximum value 1030MPa, and then decreases obviously after temperature is over 850°C as shown in Fig.3. The 0.2% offset yield stress for [111] is higher than the value for [001] and [011] orientation at room temperature, whereas reverse result obtained with temperature increase. It shows similar variation of *UTS* in Fig.4.

2. 2 Experimental Procedures

Stress rupture experiments were conducted on a creep-testing machine under different tensile stress levels at temperatures of 980°C and 1070°C. Specimens were heated with a radiation furnace to maintain the temperature gradient within ±3°C. Temperature control was achieved by using a Pt/Pt 13% Rh thermocouple, attached to the specimen in the centre of the gauge length coupled to a temperature controller. Two further thermocouples were mounted at the ends of the gauge length to monitor the test temperature.

Some of the specimens, crept at a temperature of 980°C under a constant tensile stress of 260MPa, were tested until failure or interrupted at 5, 20 and 100h, respectively. The specimens were then sectioned within gauge section either perpendicular or parallel to the axis of the specimens. The thus obtained slices of about 0.2mm thickness were thinned mechanically and polished by a twin jet polisher at -10°C and 20V to form foils for transmission electron microscope

(TEM) observations. TEM observations were conducted through JEOL 2000FX facility.

3. Results and discussions
3. 1 Microstructural evolution during creep

In order to observe the microstructural evolution during creep/rupture process, which is useful to characterize the stress rupture property of the single crystal superalloy, creep tests were conducted at a temperature of 980°C under a constant tensile stress of 260MPa. The specimens were crept to failure or interrupted at 5, 20 and 100h, respectively. Fig.5 shows the changes of creep strain with creep time increasing. The alloy exhibited a very short period of decreasing strain rate of primary stage, a relatively short steady-state stage, and a long increasing strain rate of tertiary stage at 980°C/260MPa, while no apparent incubation period was observed. The primary, secondary and tertiary stages fall in ranges from 0h to about 2h, from about 2h to about 50h and from 50h to rupture.
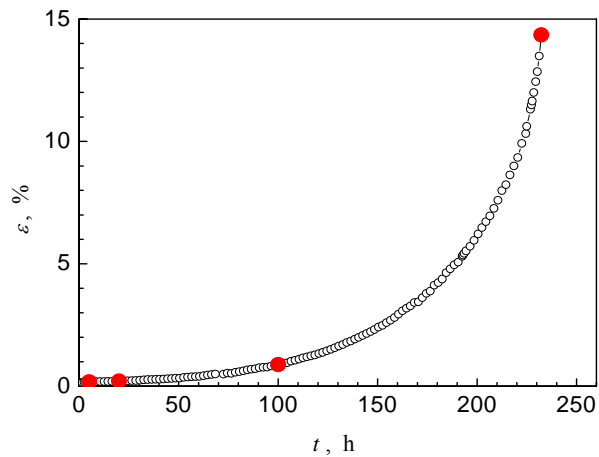
Fig. 5. Creep strain curve of the alloy with [001] orientation   at 980°C/260MPa

TEM observations were performed to characterize the features of microstructure and its evolution. Fig.6 shows the TEM micrographs of the cross section of the specimens crept for 5h, 20h and 100h as well as to rupture, respectively. Moreover, Fig.7 shows the TEM micrographs of the longitudinal section of the specimens crept in 5h and 20h as well as ruptured, respectively.

It can be concluded from these micrographs shown in Fig.6 and Fig.7 that (i) γ' particles gradually changed their shape, i.e. they were rafted; (ii) the rafted γ' may be a plate-shaped structure parallel to the cross section of specimen or a bar-shaped structure perpendicular to the cross section of specimen. However, it can be inferred that only the former case may be possible by comparing cross-section sizes of γ' particles shown in Fig.6 and the corresponding one in Fig.7.

During this creep process, there is a general non-directional γ'-coarsening, which is driven by the tendency to decrease the overall γ/γ'-interface energy of the system, and a directional γ'-coarsening, which is driven by the tendency to

4

compensate for the lattice misfit. The lattice misfit may be defined as the difference between lattice constant of an ordered γ' phase and that of a γ phase or $\delta=2(a\gamma'-a\gamma)/(a\gamma'+a\gamma)$. Due to the general non-directional γ'-coarsening, γ' particles tends to dissolve or diffuse their parts having bigger specific surface area, such as corners or edges of particles, to compensate smooth parts, such as faces of cubes. As a result, the cubic γ' particles change to ellipsoid-shaped ones. By virtue of directional γ'-coarsening, γ' particles grow up perpendicular to the stress axis and are gradually linked to form plate structure. With the progress of this rafting process, all of the γ' particles are eventually combined to continuous bodies with original γ channel being isolated to be discontinuous ones.

(a) Crept for 5h   (b) Crept for 20h

(c) Crept for 100h   (d) ruptured specimen
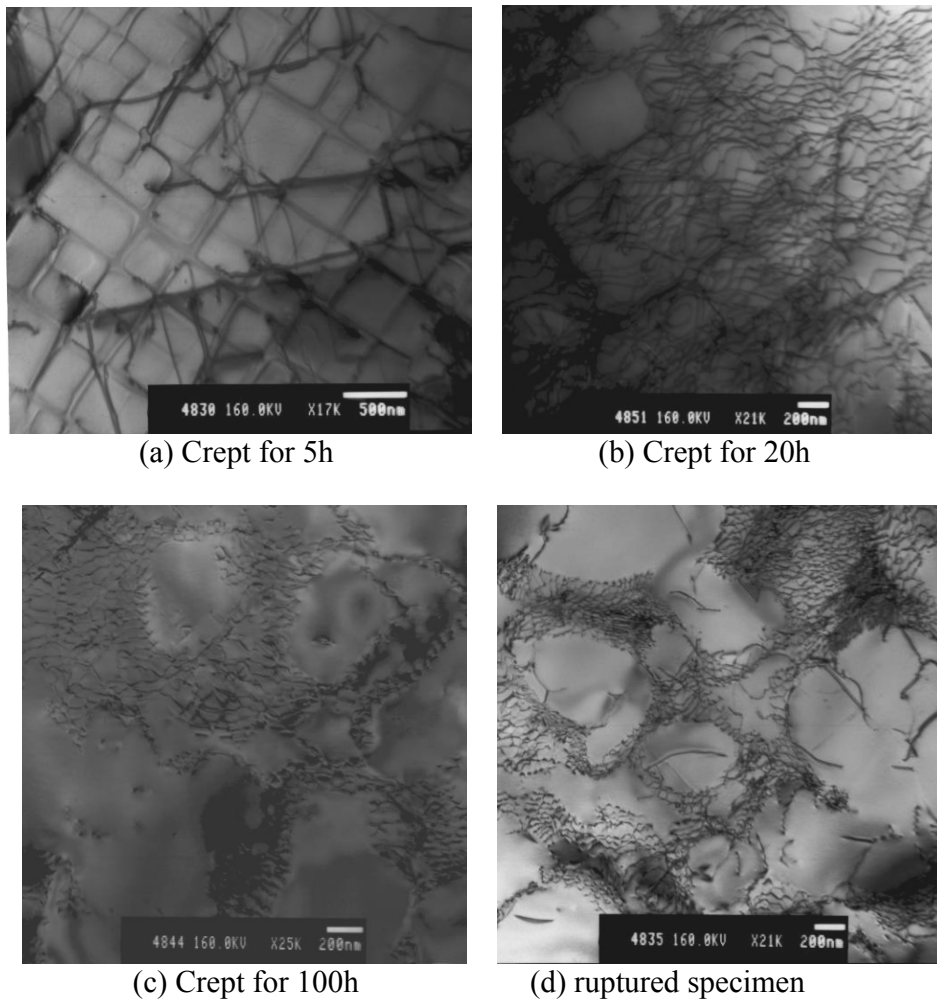
Fig. 6. Characteristic features of dislocations on cross section at different test time

Such a structure transition is very important for the creep resistance of the alloy since that, due to intrinsic characteristic of superlattice structure hard to be cut by dislocations of γ' phase, γ phase generally accommodates most of dislocations as well as movement contributing to deformation of creep. Therefore, the discontinuous structure of γ phase during creep process may exhibit a significant

obstacle to movement of dislocations therein. Fig. 7 (c) shows that dislocations in γ phase are blocked near γ/γ′ boundaries and the density thereof become higher than that in parts away from the boundaries. The hardening process may be also confirmed, to some extent, from Fig. 5 which shows that rafted structure can sustain such a long period of time of tertiary stage before its failure.

(a) Crept for 5h

(b) Crept for 20h
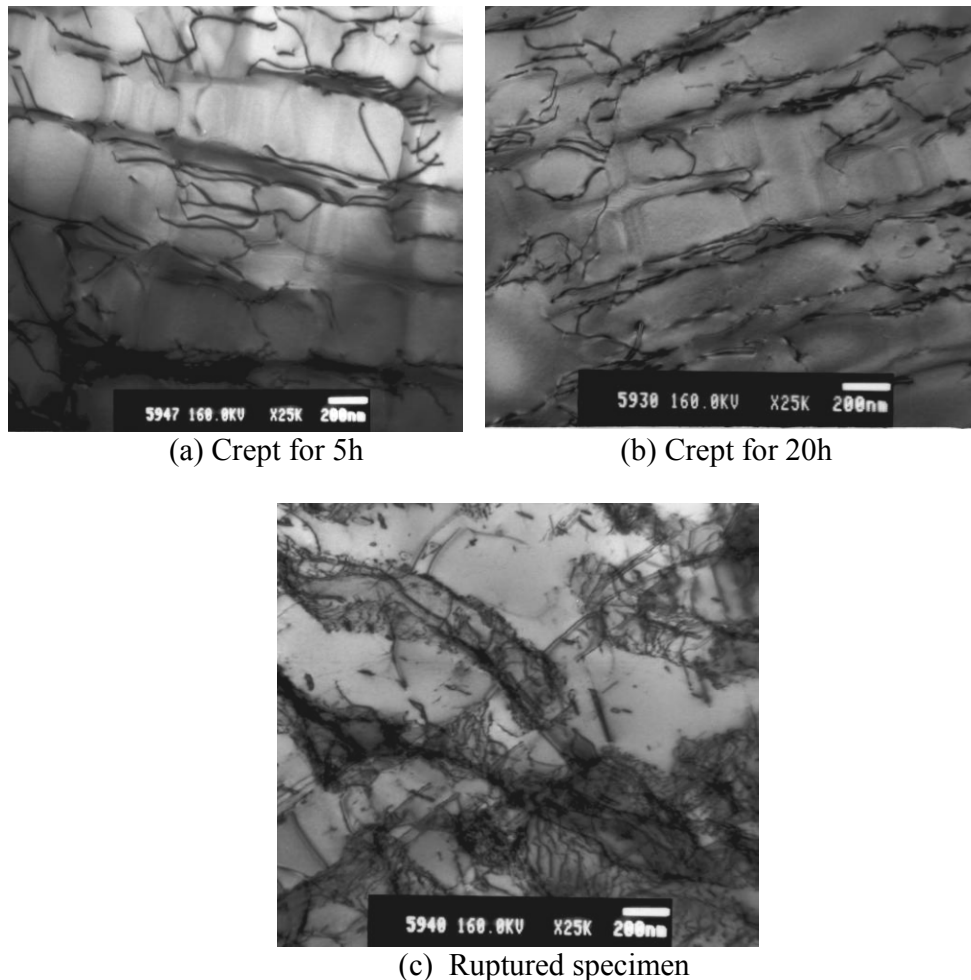
(c) Ruptured specimen
Fig. 7. Characteristic features of dislocations on longitudinal section at different test time

On the other hand, Fig. 6 (a) and Fig. 7 (a) show that no obvious rafting occurred in the 5h interrupted specimen. Referring to Fig.5, this specimen contains full of the primary stage, so the deformation of the alloy crept at this testing condition is not characterized by the rafting, but the shearing and accumulation of γ and γ′ phases by long dislocations. It is a general consensus that these dislocations are separated by intrinsic and extrinsic stacking faults combining to give an overall Burgers vector a<112> [5, 6]. The deceleration of the creep rate in primary stage may be related to the increase of the dislocation density since that dislocation slip mechanism dominates the deformation of this stage and high-density dislocations may form obstacle to further movement. At a time in a range between 5h and 20h,

the dislocation density in γ phase is saturated due to the equilibrium of multiplication and vanishing of dislocations; after that, the dislocation density keeps substantially constant until the rupture of the specimen. The rafting or diffusion mechanism dominates the remaining stages.

The creep process of this type alloy may be divided into two different stages, one is initial stage characterized by dislocation slip and the other is rafting stage characterized by rafting of γ′ phases. Both of these two stages can be unified to contribute to the damage of the alloy during creep, as described in the modeling of the stress rupture life of the alloy in the following part.

3. 2 Rupture behaviors of the alloy

The stress rupture test data for the single crystal alloy with [001], [011] and [111] orientations are illustrated in Fig. 8. The results indicate that temperature has great influence on the stress rupture life for specimens with three orientations at temperatures of 980°C and 1070°C. The stress rupture life decreases by almost 50% when the testing temperature increases from 980°C to 1070°C. The reason may be that some of the strengthening mechanisms, such as particle strengthening, may be weakened due to the bypassing and climbing of dislocations when the testing temperature reach to 980°C and higher.
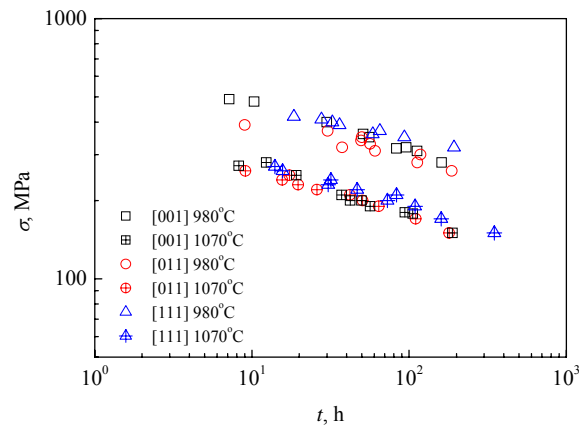
Fig. 8. Stress rupture data of a single crystal superalloy with different orientations at 980°C and 1070°C

At 980°C, the stress rupture strengths of the alloy with [001] and [111] orientations are nearly the same, which are some superior to that with [011] orientation. However, comparing to the short time UTS, the stress rupture strengths of the alloy with three orientations are not so different. In contrast, the short-time UTS of the alloy with three orientations are very different as shown in Fig.4. At 1070°C, there are no much differences of stress rupture strength with three orientations. During a short time tensile process, slip mechanism, depending largely on orientation, controls the deformation while no obvious diffusion occurs. But during a creep process at temperature of 980°C or higher, diffusion mechanism dominates the creep deformation, which is a temperature-dependent process. Such transition of deformation mechanisms may be the cause of less

differences of stress rupture strength with different orientations at higher temperature.

3. 3 Stress Rupture Life Modeling

Damage mechanics has been widely used to characterize the microstructural evolution that occurred during the creep process, in which a state variable ω is a measure of change from initial state. Kachanov [7] proposed a function for brittle viscoplastic damage occurring during polycrsytalline alloys as follows:

$$\frac{d\omega}{dt} = f(\sigma, T, \omega) \qquad (1)$$

where σ is the applied stress, T is testing temperature and ω is a damage-state variable. For isothermal conditions, the function chosen for f in Eq. (1) was of power form according to reference [7]:

$$\frac{d\omega}{dt} = C(\frac{\sigma}{1-\omega})^v \qquad (2)$$

where C and v are material constants. Eq. (2) can be integrated for constant σ between the limits $\omega=0$ at $t=0$ and $\omega=1$ at $t=t_r$ to give the following expression for rupture life:

$$t_r = \left[C(v+1)\sigma^v\right]^{-1} \qquad (3)$$

where t_r is stress rupture life. However, Eq. (3) implies a straight line relationship between stress and rupture life, plotted on log scales, which is appropriate for low stress long time brittle failure of polycrystalline, not for testing conditions of this study.

MacLachlan [8] modeled stress rupture life data by combining short time tensile property to creep data with the following form:

$$t_r = \frac{1}{C \times (v+1) \times UTS} \times \frac{(UTS - \sigma)^{(v+1)}}{\sigma^v} \qquad (4)$$

where UTS is ultimate tensile strength of material. However, this equation cannot reflect features of the short time tensile property enough, so the applicability of this method is also relatively poor.

On the other hand, the above method considers the initiation and growth of microcracks form the pre-existing casting porosity occurring at interdendritic region as a significant form of creep damage. However, according to the TEM analysis of this study, creep damage occurs not only during the rafting or microcrack initiation process, but also during the primary stage of creep process. On the basis of above consideration, a modified method is derived to quantify the stress rupture data of this type alloy as follows:

$$t_r = C[\frac{(UTS - \sigma)(UTS - \sigma_{0.2})}{E}]^v \qquad (5)$$

where E is elastic modulus, $\sigma_{0.2}$ is 0.2% offset yield stress, C and v are material constants depending on the temperature. In Eq.(5), the expression of $(UTS-\sigma)(UTS-\sigma_{0.2})/E$ is taken as a damage parameter during creep process to describe the creep damage per unit time, then time till failure is a function being of power form with the damage parameter. When using Eq. (5), the level of damage caused failure occurs when the applied stress reach UTS. Moreover, this model reflects

the fact that the stress rupture life tends to be more sensitive to the applied stress when the relative difference between $\sigma_{0.2}$ and UTS is rather small.
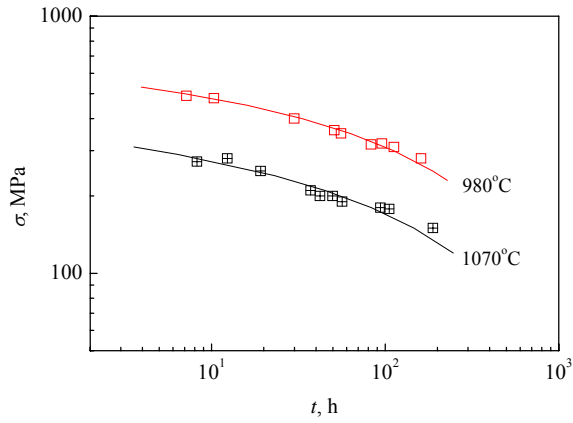
Fig.9. Stress rupture data of the single crystal superalloy with [001] orientation.
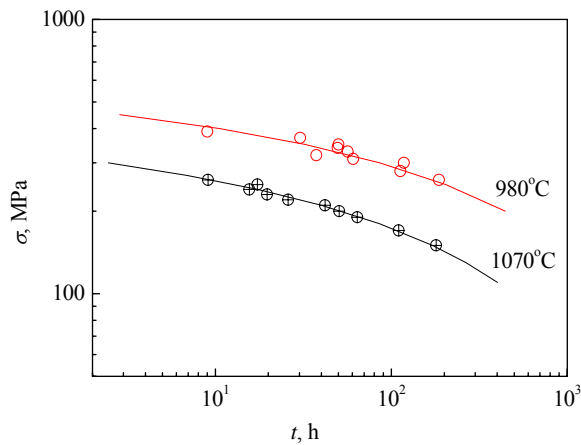
Fig.10. Stress rupture data of the single crystal superalloy with [011] orientation.
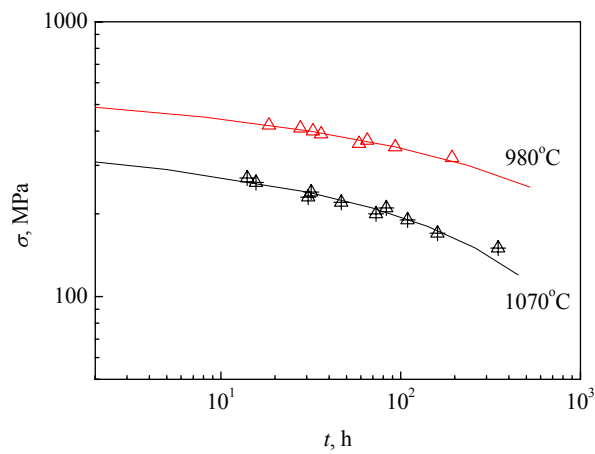
Fig. 11. Stress rupture data of the single crystal superalloy with [111] orientation.

Stress rupture data of the alloy with three orientations are shown in Fig.9 to Fig.11. The calculated results by Eq. (5) are also plotted in Fig.9 to Fig.11. It can be observed that the predications of this method are consistent with the testing data very well, and the disadvantage of straight line relationship between stress and rupture life which is proposed by some conventional damage mechanics theory is overcome since that the damage parameter is related to not only the applied stress but also the short-time tensile properties of the alloy.

4. Conclusions

(1) Creep process of this SC alloy may be divided by two different stages, one is initial stage characterized by dislocation slip and the other is rafting stage characterized by rafting of γ′ phases. Both of the two stages are contribute to the damage of the alloy during creep.

(2) The single crystal nickel base superalloy with [001] and [111] orientations exhibited superior stress rupture life to [011] orientation at 980°C, but the differences among long-time stress rupture strength at 1070°C are relatively small.

(3) A damage parameter was deduced on the basis of the quantitative relationship between applied stress and the short-time tensile property. It can model the stress rupture properties of single crystal nickel base superalloy with different orientations in a rather high accuracy.

References

[1] C.T. Sims, N.S. Stoloff and W.C. Hagel, Superalloys II, John Wiley & Sons, Inc, New York, 1987

[2] J.R. Davis (Ed.) Heat-Resistant Materials, ASM Specialty Handbook. The Materials Information Society, 1997

[3] S.S.K. Gunturi, D.W. MacLachlan and D.M. Knowles, Anisotropic creep in CMSX-4 in orientations distant from <001>, Mater. Sci. Eng. A289 (2000) 289-298

[4] J.R. Li, Z.G. Zhong, D.Z. Tang, Low cost second generation single crystal superalloy DD6, Acta Metallurgica Sinica 35 (Suppl. 2) (1999) S266-S269

[5] R.A. MacKay and R.D. Maier, The influence of orientation on the stress rupture properties of nickel-base superalloy single crystals, Met. Trans. 13A (1982) 1747-1754

[6] N. Matan, D.C. Cox, P. Carter, M.A. Rist, C.M.F. Rae and R.C. Reed, Creep of CMSX-4 superalloy single crystals: Effects of misorientations and temperature, Acta Matall. Mater. 47 (1999) 1549-1563

[7] L.M. Kachanov, Introduction to continuum damage mechanics, Kachanov, Martinus Nijhoff Publishers, Dordrecht, The Netherlands, 1986

[8] D.W. MacLachlan and D.M. Knowles, Modelling and prediction of the stress rupture behavior of single crystal superalloys, Mater. Sci. Eng. A302 (2001) 275-285